HIGH-TEMPERATURE FATIGUE IN METALS

Gary R. Halford
NASA Lewis Research Center
Cleveland, Ohio

INTRODUCTION

The presentation focuses primarily on the progress we at NASA Lewis Research Center have made in the understanding of the phenomenological processes of high-temperature fatigue of metals for the purpose of calculating lives of turbine engine hot section components. Improved understanding has resulted in the development of accurate and physically correct life prediction methods such as Strain-Range Partitioning (SRP) for calculating creep-fatigue interactions and the Double Linear Damage Rule (DLDR) for predicting potentially severe interactions between high- and low-cycle fatigue. Examples of other life prediction methods are also discussed.

FATIGUE LIFE PREDICTION APPROACH

The major technology areas needed to perform fatigue life predictions of turbine engine hot section component parts are shown in figure 1. The NASA Lewis Research Center has substantial efforts in each of these areas.

We begin with a determination of the operating environment and a calculation of the thermal and mechanical loading of combustor liners, inlet guide vanes, turbine blades, and disks. We then determine the cyclic stress-strain and creep behavior of the engine materials so that the finite element structural analyses can be made. The results of the analyses are the local stress strain temperature versus time response of the material at the most critical locations in the component part. Finally, from a knowledge of the fatigue, creep, and fracture resistance of the materials, we can make a prediction of the lifetime of the component part.

The presentation will focus primarily on the progress we at NASA Lewis have made in the areas of material characterization and failure analysis for the purpose of calculating turbine engine hot section component fatigue and thermal fatigue lives. We have recognized for many years that our fatigue research has applicability beyond the aeronautical and space arenas, and have maintained an interface with other industries in order that they may benefit in some measure. This conference is another example of our desire to share the fruits of our research.

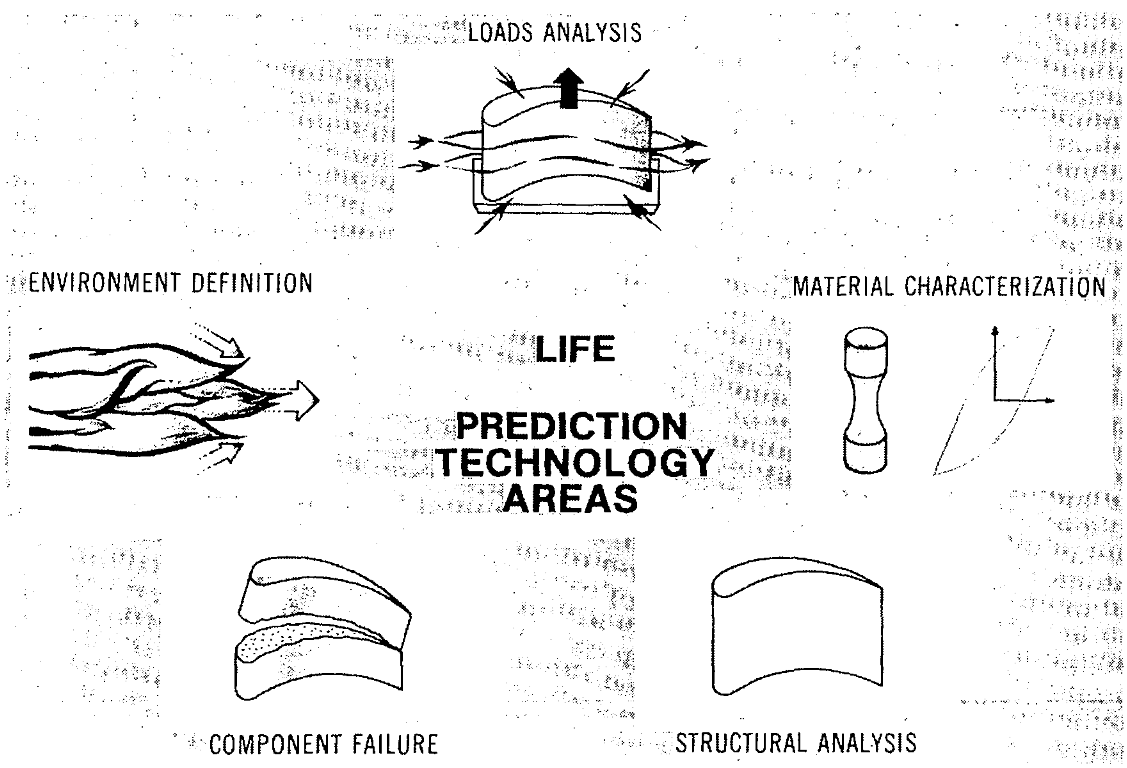

Figure 1

LIFE PREDICTION PROBLEMS IN ENGINE HOT SECTIONS

The specific problem areas within the hot section are shown in figure 2. Typical modes of failure are listed for each of the components that suffer degradation during engine operation.

Combustor liners -- Thermal fatigue and creep buckling

Seals -- Wear

Disks -- Low-cycle fatigue

Vanes and Blades -- Thermal low-cycle fatigue and chemical attack

With the exception of the centrifugal loads on the blades and disks, the primary source of cyclic fatigue loading is due to the severe thermal cycling associated with each startup and shutdown of the engine, although high-frequency excitation problems are sometimes encountered.

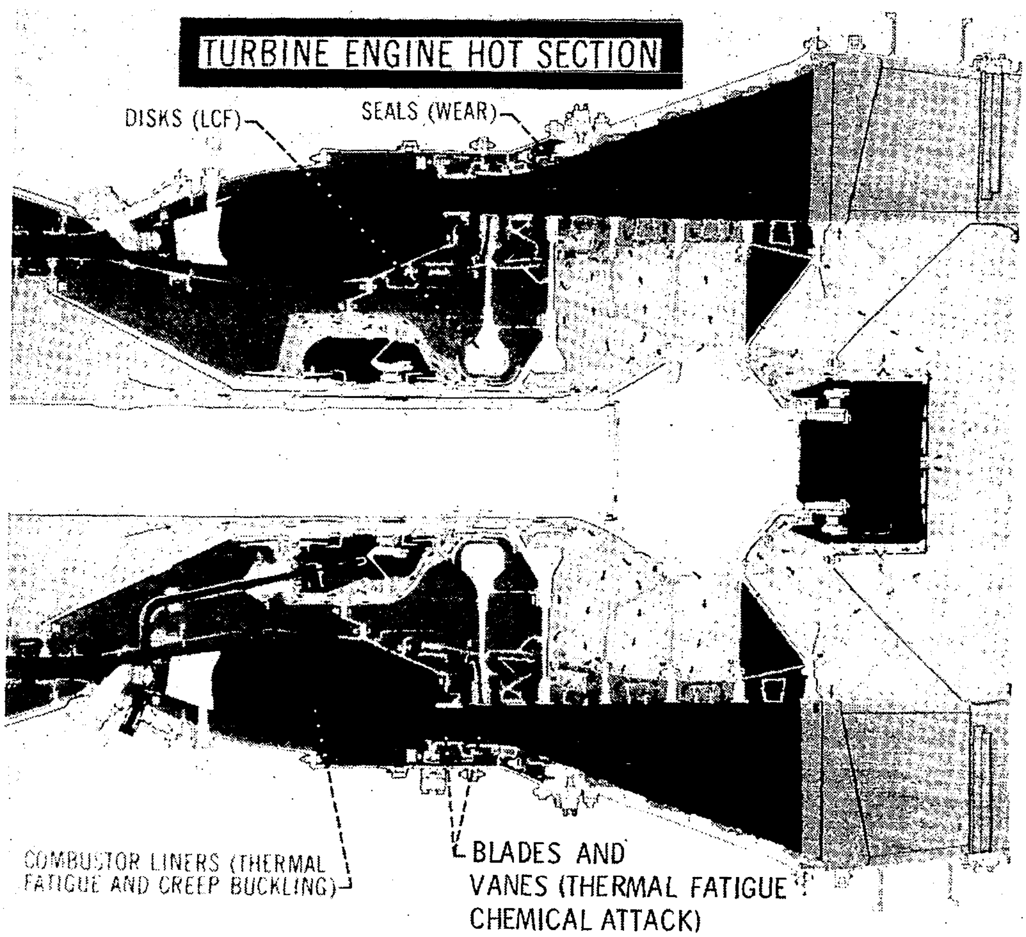

Figure 2

LOW-CYCLE THERMAL FATIGUE

Low-cycle fatigue and thermal fatigue occur in component parts where the strain in a small localized region is larger than in the surrounding region because of notches that concentrate the strain, or because of constrained thermal expansion as in the case of thermal fatigue. The key feature is that the local strain is prevented from exceeding certain bounds because the bulk of the component part remains elastic. Hence, the local material is caused to cycle between approximately constant strain limits. When the local strains are large, inelastic strains occur and the cyclic stress-strain behavior becomes nonlinear with a hysteresis loop forming, as shown schematically in figure 3. Note the terms used to describe the characteristics of the hysteresis loop. The stress range, $\Delta\sigma$, and the elastic strain range, $\Delta\varepsilon_e$, are related by the modulus of elasticity, E. The total strainrange, $\Delta\varepsilon$, is the sum of the elastic strainrange, $\Delta\varepsilon_e$, and the inelastic strainrange, $\Delta\varepsilon_{in}$.

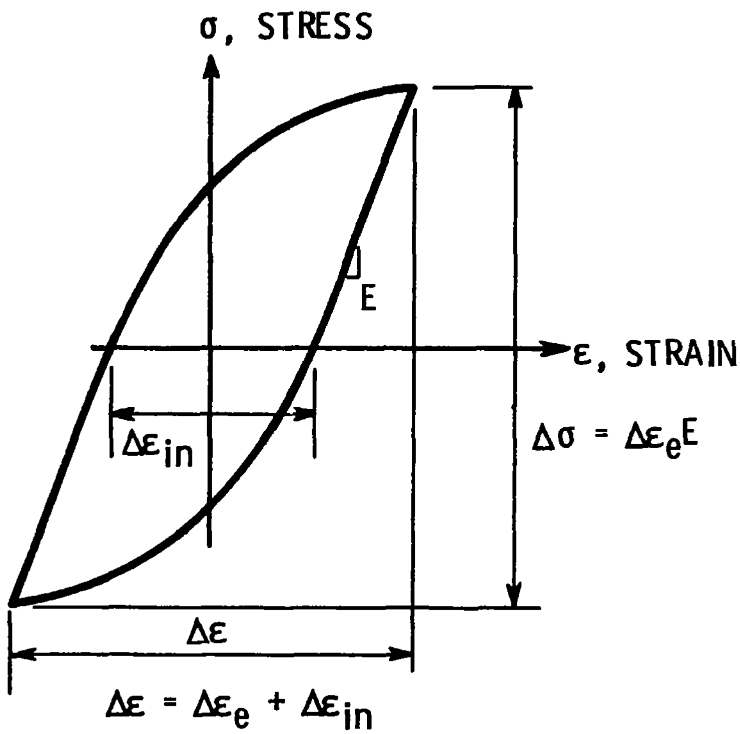

Figure 3

HOW DO WE ATTACK THIS PROBLEM?

To study the problem of large cyclic strains, it was necessary to evolve an entirely new testing philosophy and to develop new testing equipment. To measure the cyclic stress-strain and low-cycle fatigue behavior of materials at large strains, axially loaded, strain-controlled testing was required. Consequently, cyclic strain extensometers were developed for measuring and controlling the inelastic strains encountered during testing. Closed loop, servocontrolled testing machines were designed, built, and perfected. A closeup view of a resistance heated, axially loaded, elevated temperature specimen is shown in figure 4. An extensometer measures the change in diameter of the round bar specimen. The sensing element is a linear variable differential transformer. Strains as small as 20 microinches per inch can be detected with this device.

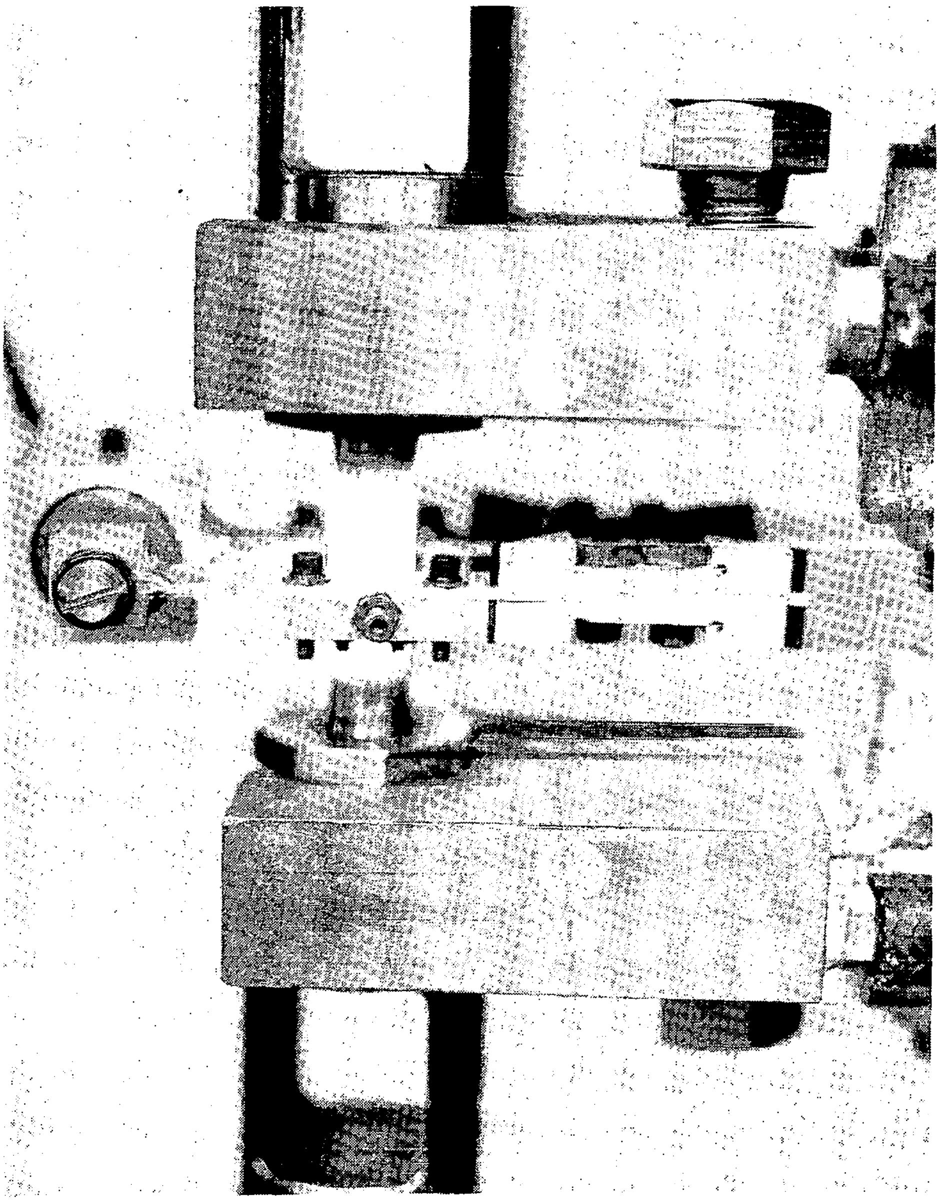

Figure 4

Figure 5 serves to illustrate that the cyclic strainrange is used to correlate the low-cycle fatigue resistance of alloys. Results of low-cycle fatigue tests are displayed on logarithmic coordinates of strainrange versus cycles to failure. Note that the total strainrange curve is asymptotic to the inelastic strainrange curve at very low cyclic lives and is asymptotic to the elastic strainrange curve at long cyclic lives. As indicated earlier, the total strainrange is simply the sum of the elastic and inelastic strainranges. For most materials, the elastic and inelastic strainrange curves are straight lines on the logarithmic coordinates. This representation of fatigue behavior is usually valid up to 10^6 cycles to failure.

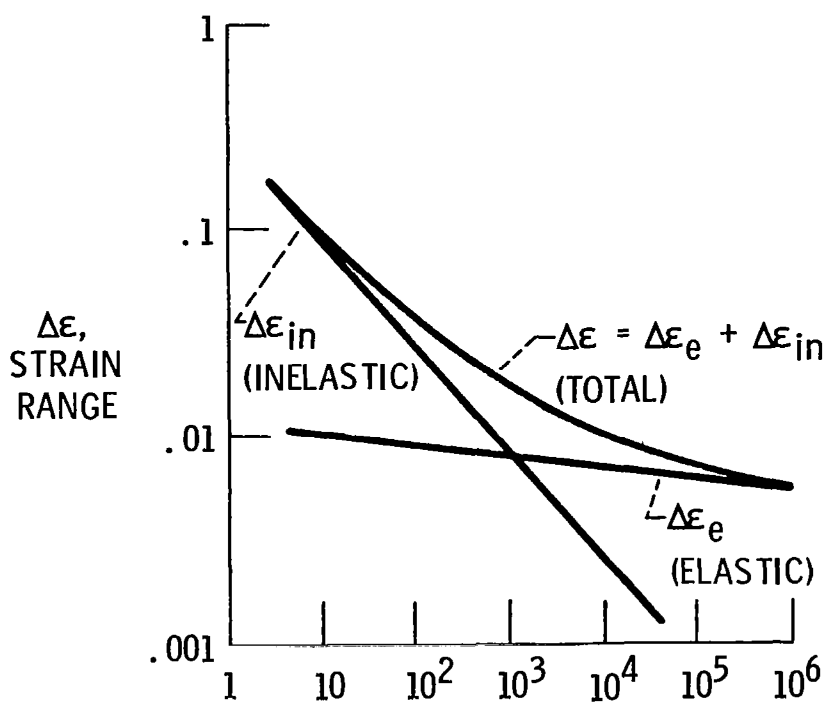

Figure 5

MANSON-COFFIN LAW FOR LOW-CYCLE FATIGUE

With that introduction, I would like to now present a brief historical overview of the contributions made by NASA Lewis engineers in the development of material life prediction methods for low-cycle and thermal fatigue. Our first contribution came in the early 1950's when S. S. Manson (now a professor at Case Western Reserve University) first proposed the power law relationship between the inelastic strainrange and cycles to failure (ref. 1). This law has come to be known as the Manson-Coffin Law for low-cycle fatigue. It expresses the observation that for almost all materials, at room temperature, the slope of the logarithmic straight line is constant (see fig. 6). Furthermore, the coefficient "C" is related to the ductility measured in a tensile test. The greater the ductility, the greater is "C". The Manson-Coffin Law served to provide a better understanding of what causes the fatigue process (reversed crystallographic slip with properly oriented crystals of the metal). However, to apply the law to the prediction of low-cycle fatigue life required that the inleastic strainrange in a component part be known accurately. At the time, the technology was lacking for calculating inelastic strains in a component part. Hence, a more practical approach was needed.

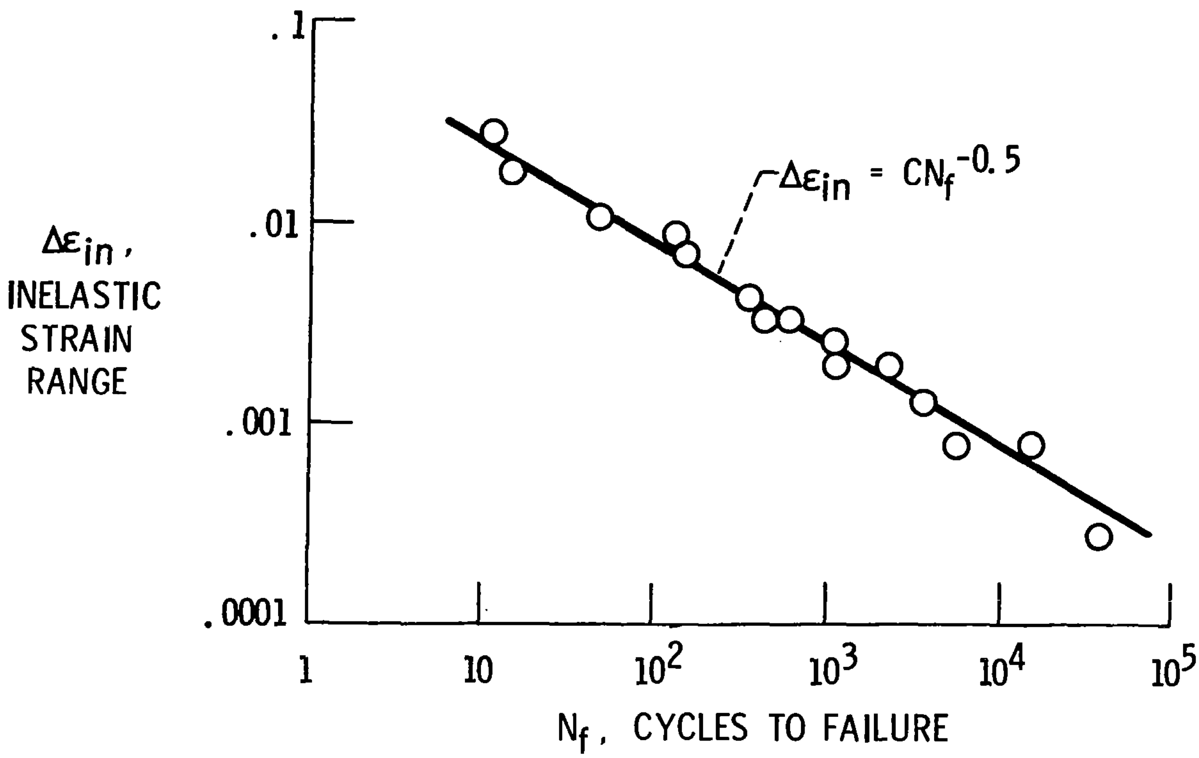

Figure 6

UNIVERSAL SLOPE METHOD FOR ESTIMATING FATIGUE LIFE

Although the inelastic strainrange could not always be calculated accurately, the total strain could be by using the concept of strain invariance along with an elastic stress analysis. Thus, by expressing the low-cycle fatigue resistance of a material in terms of total strainrange versus cycles to failure, practical predictions of life could be made. In 1964, Manson and Hirschberg (ref. 2) recognized the importance of this viewpoint and developed a procedure for representing the low-cycle fatigue curves in terms of the total strainrange. Then, they proposed a procedure for estimating the total strainrange versus cycles to failure curve from only a knowledge of a material's tensile test properties. Their method was called the Method of Universal Slopes since it assumed a constant slope of -0.12 for the elastic line and a constant slope of -0.60 for the inelastic line (see fig. 7). Furthermore, the intercept of the elastic line was related directly to the σ_u (ultimate tensile strength) and the E (modulus of elasticity) of the material. The intercept of the inelastic line was related to D (the ductility in a tensile test). The approach was an immediate success and is used widely during preliminary design.

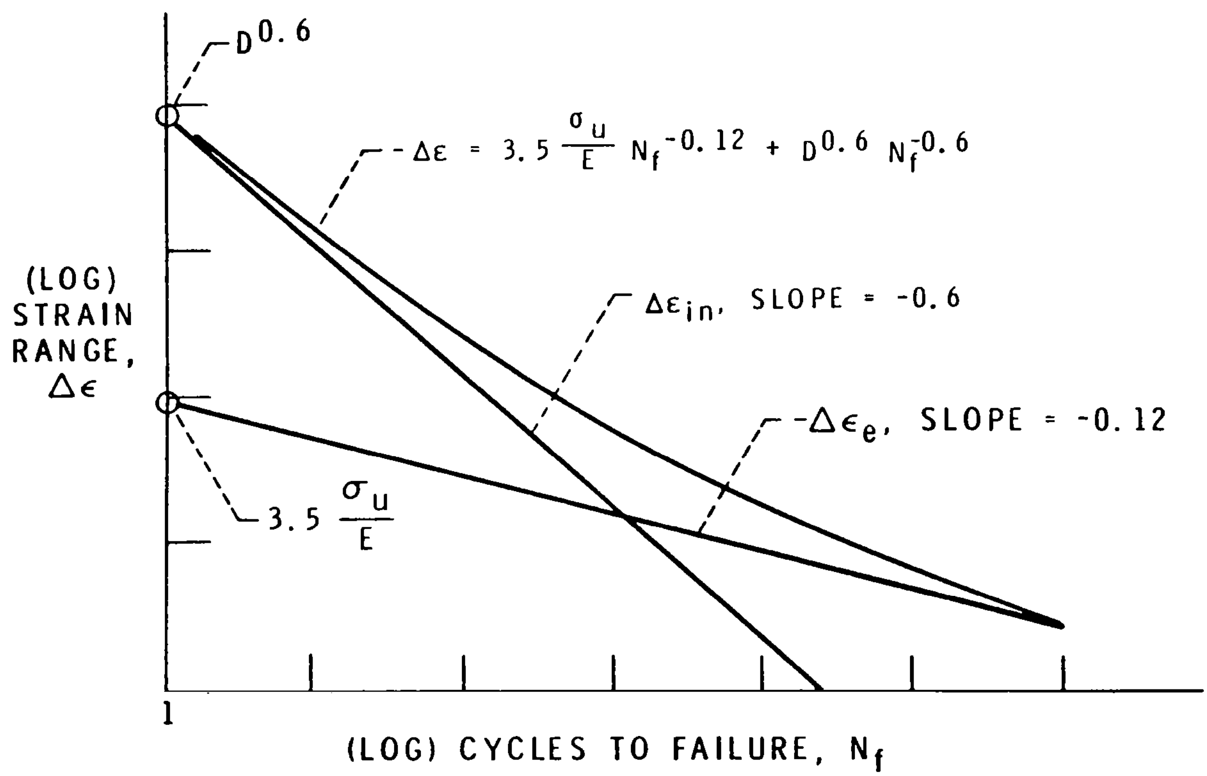

Figure 7

PREDICTIVE CAPABILITY OF METHOD OF UNIVERSAL SLOPES

As seen in figure 8, the Method of Universal Slopes (ref. 2) follows the trend of low-cycle fatigue data reasonably well over a range of six orders of magnitude in cyclic life. For any given material, the predicted cycles to failure may be wrong by as much as a factor of ten in the extreme. However, this uncertainty is usually acceptable considering the fact that fatigue tests are not required -- only materials tensile properties are needed to estimate the fatigue behavior. Since the Method of Universal Slopes was developed on the basis of low-temperature data, its applicability to high-temperature, low-cycle fatigue was in question.

First attempts to apply this method at high temperatures, using high-temperature tensile properties, resulted in overpredictions of life. The cyclic lives were lower than expected because at the high testing temperature, detrimental attack of the material grain boundaries occurred from oxidation and cyclic creep strain. Short-time tensile properties were unaffected by these factors and hence were no longer directly appropriate for use in estimating cyclic lifetimes.

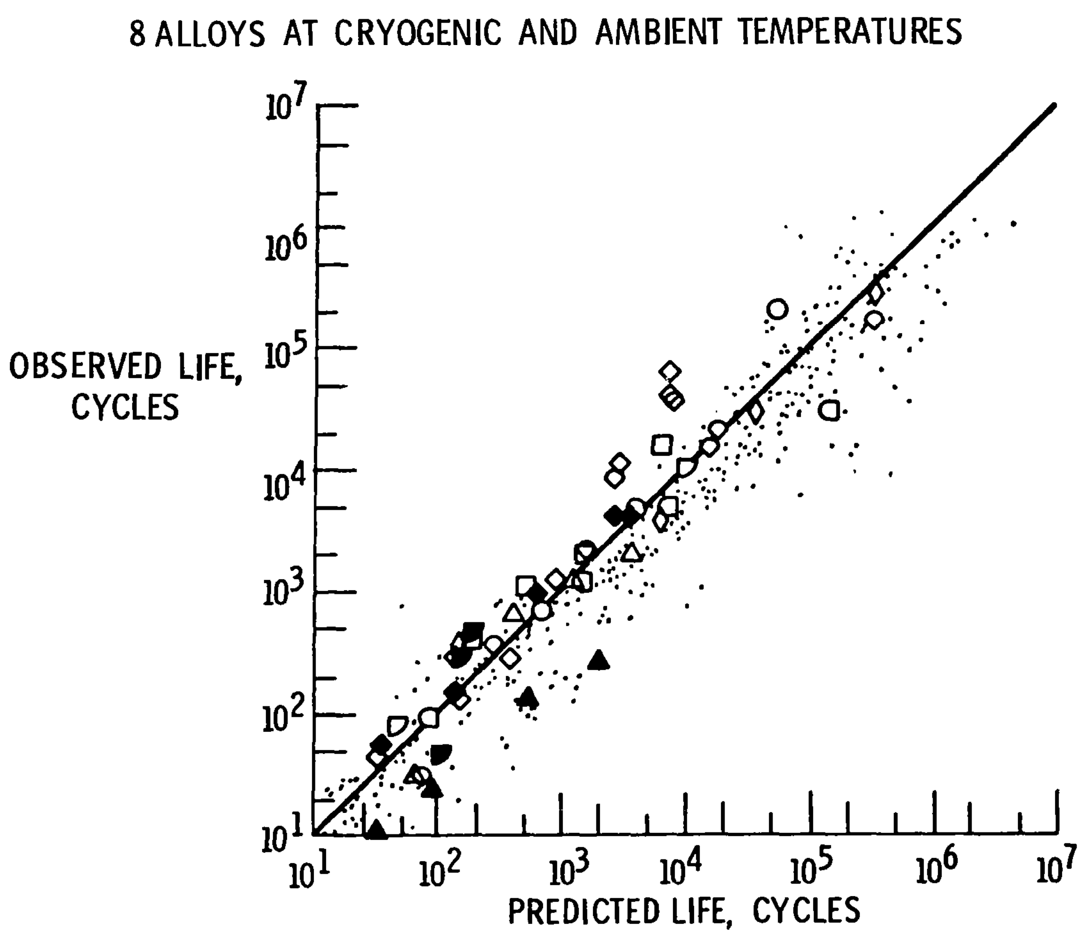

Figure 8

10% RULE FOR PREDICTING HIGH-TEMPERATURE LOW-CYCLE FATIGUE

As a first approximation to the effects of grain boundary attack on the fatigue process, it was recognized that the micro-crack initiation process was being bypassed, leaving only the crack propagation portion of the total life. Since the propagation life could be as low as about 10% of the total life in low-cycle fatigue, it was reasoned that an estimate of the minimum high-temperature low-cycle fatigue behavior of a material could be taken as equal to 10% of the life calculated by the Method of Universal Slopes (fig. 9). This rule referred to as the "10% Rule" was proposed in 1967 by Manson and Halford (ref. 3) and applied to all of the high-temperature low-cycle fatigue data available at the time.

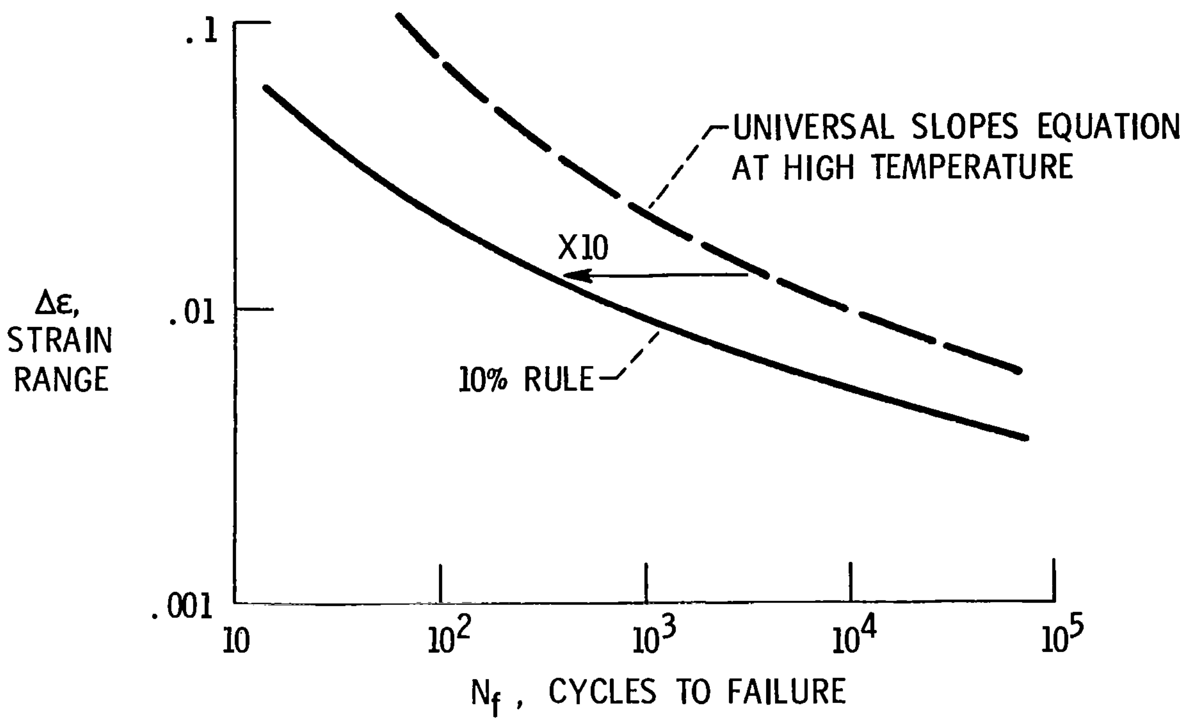

Figure 9

PREDICTIVE CAPABILITY OF 10% RULE

As seen in figure 10, we were able to verify that the method did indeed predict the trends in the available data over the range of 10 to 10^5 cycles to failure. The accuracy of the predictions was on the same order as the accuracy of the Method of Universal Slopes for lower temperature fatigue. Because of the method's simplicity, it has been used on many occasions when no high-temperature low-cycle fatigue data were available, but high-temperature tensile properties were. However, it did not account for details of a high-temperature cycle which have since been found to be important. Some of these details are: Frequency, Hold Times, Temperature, and Cycle Wave Shape.

Thus, we were motivated to seek a high-temperature life prediction method that could account for these important cycle details. The Time and Cycle Fraction Method that Professor Taira of Japan had been working on (ref. 4) possessed some of the desirable features we were looking for.

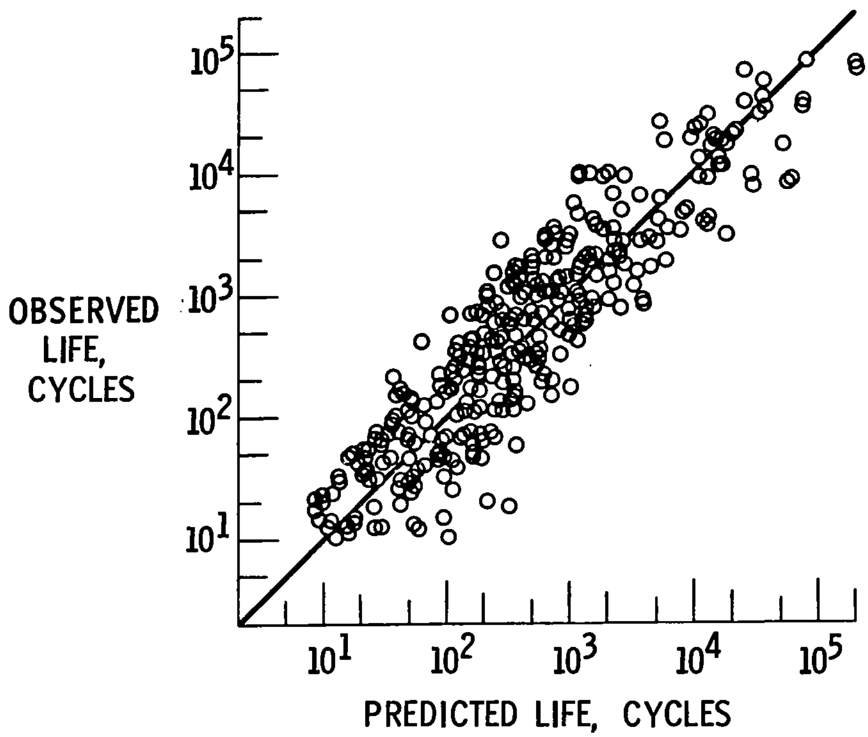

Figure 10

TIME AND CYCLE FRACTION METHOD

We made modifications (ref. 5) to Taira's method to make it more appropriate to low-cycle fatigue life prediction. Creep damage and fatigue damage are calculated independently, then the damages are summed linearly. Failure is predicted to occur when damage reaches 100%. Creep damage is expressed as a life fraction, that is, the ratio of the time spent at a stress divided by the time to rupture at that stress. Similarly, the fatigue damage is expressed as a life fraction determined from the number of cycles applied at a given total strain range divided by the number of cycles to failure at that strain range in a high-frequency fatigue test. The final expression for predicting the lifetime of any creep-fatigue cycle is indicated at the bottom of figure 11.

Although the method does have the capability to handle frequency, hold time, and temperature effects on the expected cyclic lifetime, the method does suffer limitations. Notable among these are that, (a) Creep damage is highly sensitive to stress, thus highly accurate stress calculations are needed. This is difficult to accomplish under high-temperature high-strain loading conditions, (b) Compressive creep damage is difficult to define since compressive creep rupture does not occur, yet compressive cyclic creep damage does, and (c) The method does not build in any synergistic effect of creep on fatigue or fatigue on creep.

Because of these limitations, we sought a more unifying framework for predicting cyclic lifetime under creep-fatigue conditions.

FAILURE MODE	STRESS-TIME-DEPENDENT	STRAIN-CYCLE-DEPENDENT
FAILURE CRITERION	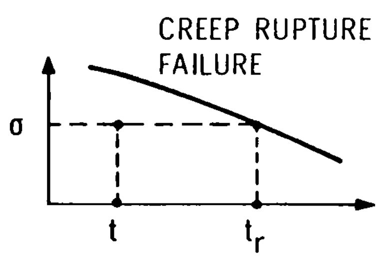	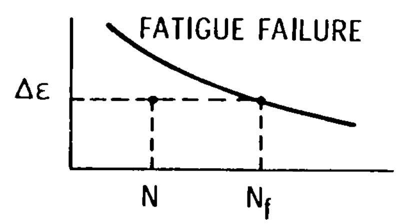
MEASURE OF DAMAGE	LIFE FRACTION t/t_r	LIFE FRACTION N/N_f
ACCUMULATION OF DAMAGE	LINEAR SUMMATION TO 1 $\sum \frac{t}{t_r} = 1$ (AT FAILURE)	LINEAR SUMMATION TO 1 $\sum \frac{N}{N_f} = 1$ (AT FAILURE)
COMBINATION	$\sum \frac{t}{t_r} + \sum \frac{N}{N_f} = 1$ (AT FAILURE)	

Figure 11

FOUR BASIC CYCLES OF SRP

In 1971, Manson, Halford, and Hirschberg (ref. 6) proposed an entirely new life prediction method that had the potential to overcome previously encountered limitations. It is a strain-based approach and recognizes the desirability of dividing (or partitioning) the inelastic strain into its creep and plastic strain components. The creep strain is thermally activated, diffusion controlled, and is the time-dependent portion. The plastic strain is time independent and is a result of crystallographic slip within metallic grains. The two basic types of inelastic strain can then be combined in the two directions of uniaxial loading -- tension and compression. This combination leads to four distinct types of cycles which are shown in figure 12. We call these the four basic cycles of Strainrange Partitioning (SRP). In a short-hand notation, these are PP (plastic strain in tension and compression), CP (creep in tension, plasticity in compression), PC (plasticity in tension and creep in compression), and finally, CC (creep in both tension and compression). Strain cycling tests can be conducted in the laboratory that feature these four types of cycles. A series of such tests conducted to failure gives the results shown schematically in the next figure.

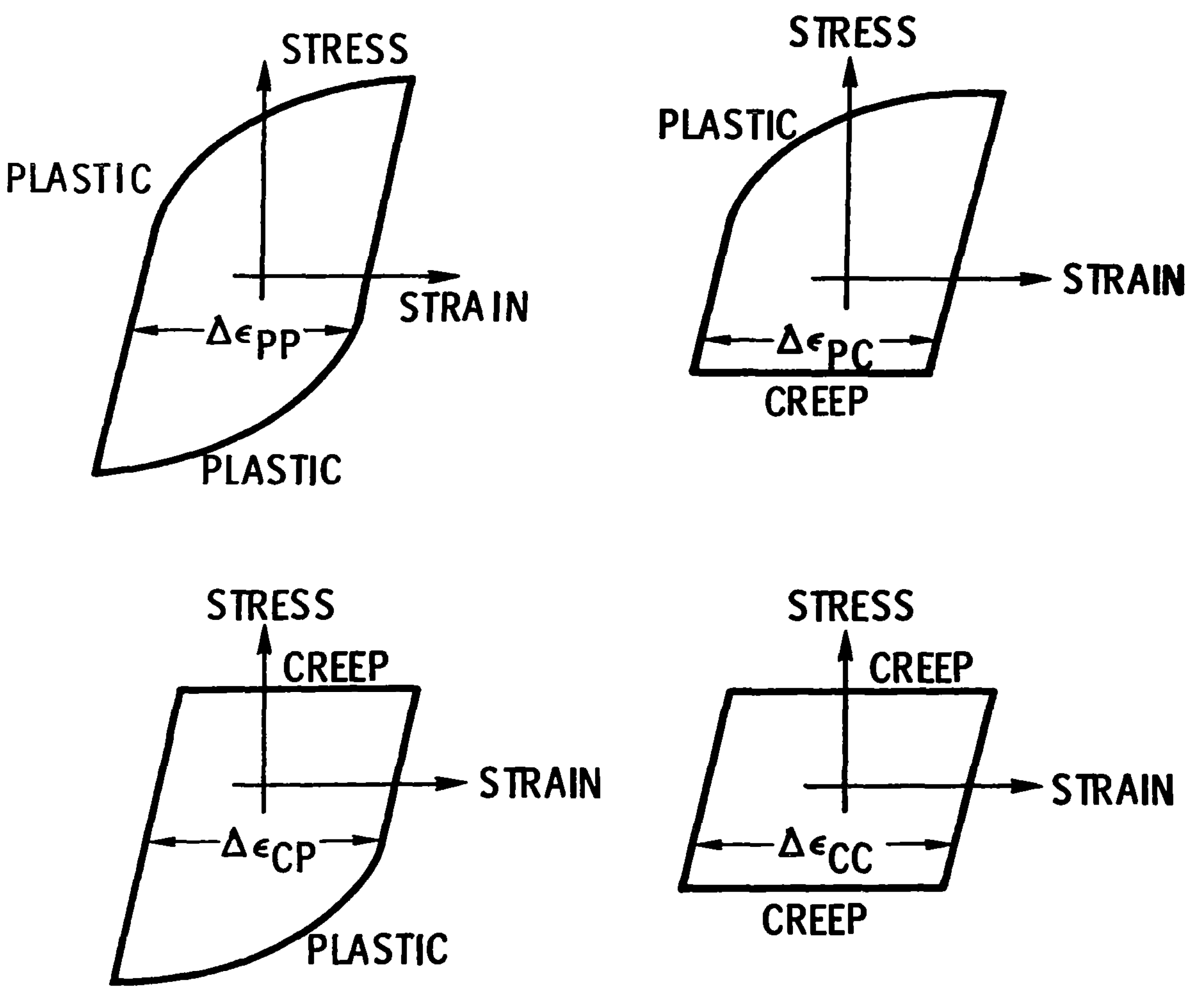

Figure 12

TYPICAL SRP LIFE RELATIONS

Each cycle type produces a unique curve of inelastic strainrange versus cycles to failure on logarithmic coordinates. These curves are called the SRP life relations. As shown in figure 13, the PP curve is usually the highest and the CP curve is usually the lowest with the PC and the CC curves being intermediate. It should be noted that these relations represent extremes in cyclic lives, and that any closed cycle is a combination of components of these types of cycles and thus will have a cyclic life that lies somewhere between these extremes.

Using the Strainrange Partitioning Method, it is possible to characterize the creep-fatigue properties of high-temperature alloys. Because the approach is generic, it is applicable to any material that undergoes high-temperature cyclic inelastic deformation, and it is applicable to any conceivable inelastic strain cycle.

A likely reason for the generality of the approach is that it is based upon a micromechanistic deformation model that is physically sound. The next figure illustrates this schematically and with photomicrographs of an alloy that has been cyclically deformed according to each of the four basic SRP cycles.

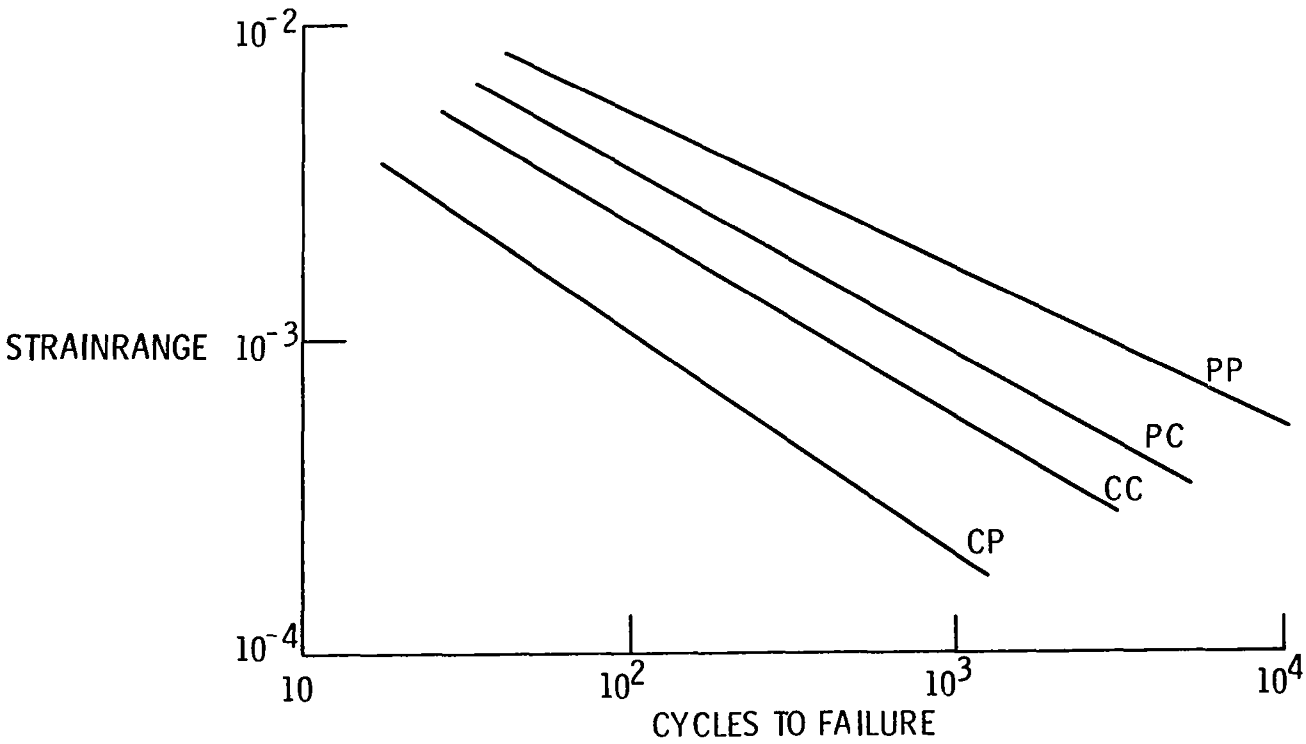

Figure 13

MECHANISMS OF SRP

A set of four simple cyclic deformation models is shown schematically in figure 14 for one complete cycle of PP, PC, CP, and CC type SRP's. Plastic strain is shown by a slip along a crystallographic slip plane while creep is shown as sliding along with a grain boundary. When these two types of strain are applied in the two directions of loading, the result is four completely different looking deformation models. The general agreement between the simple deformation model and the microstructures that develop has given credence to the validity of the SRP method of describing high-temperature creep-fatigue behavior of materials. The method has been shown to correlate the creep-fatigue behavior of a wide variety of alloys.

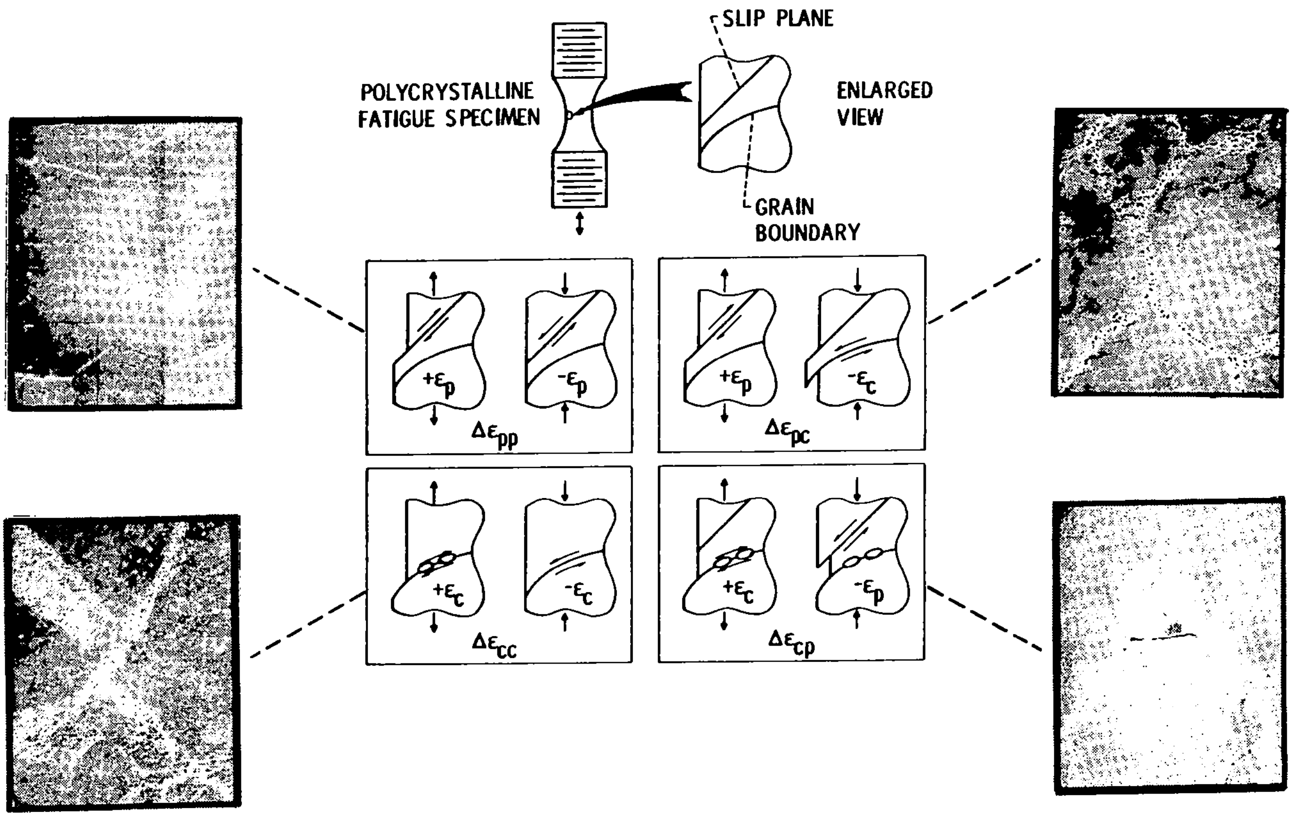

Figure 14

For a number of different materials, including nickel-, cobalt-, iron-, tantalum- and even copper-base alloys, the method of SRP has been able to correlate the cyclic life behavior of laboratory specimens to within factors of two (fig. 15). We consider this to be excellent correlation, since repeat data may vary by as much as a factor of two. For these data, there were variations in details of the cycles that the method of SRP was able to take into account. In particular, these included variations in cyclic frequency, hold times, a variety of temperatures, and of course, the cycle wave shape.

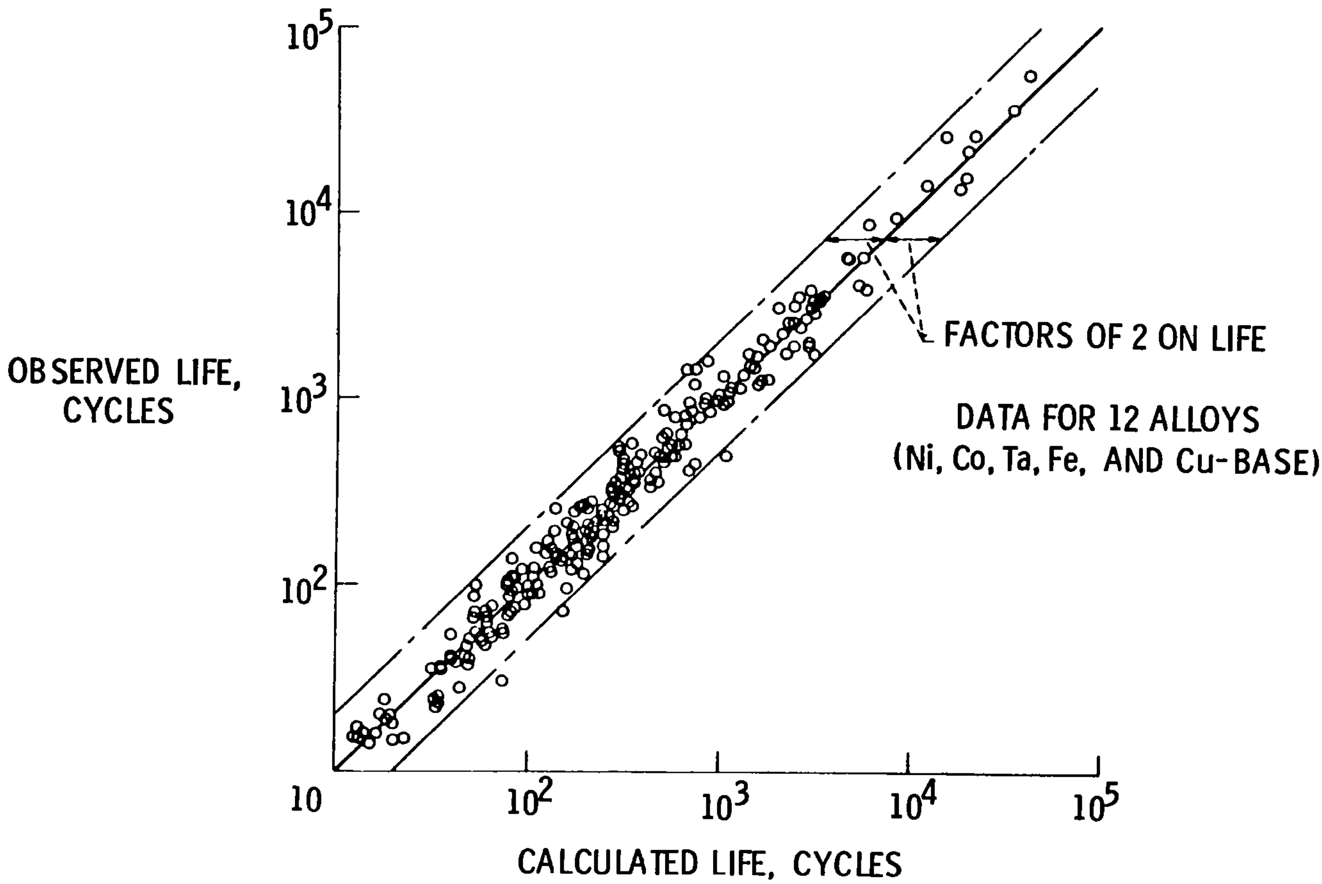

Figure 15

BOUNDS ON LIFE

In addition to correlating high-temperature, low-cycle fatigue data, the ability of the method to predict cyclic lives has also been addressed. The major advantage of the method is its ability to place upper and lower bounds on cyclic lifetime. For most materials, the PP cycle is the least damaging and gives the greatest lifetime whereas the CP cycle is the most damaging and is associated with the lowest life possible due to creep-fatigue.

The method of SRP can also predict the transition in cyclic lives between the upper bound and a lower bound as the cyclic testing frequency, for example, is reduced. A schematic is shown in figure 16 for the transition between PP and CC.

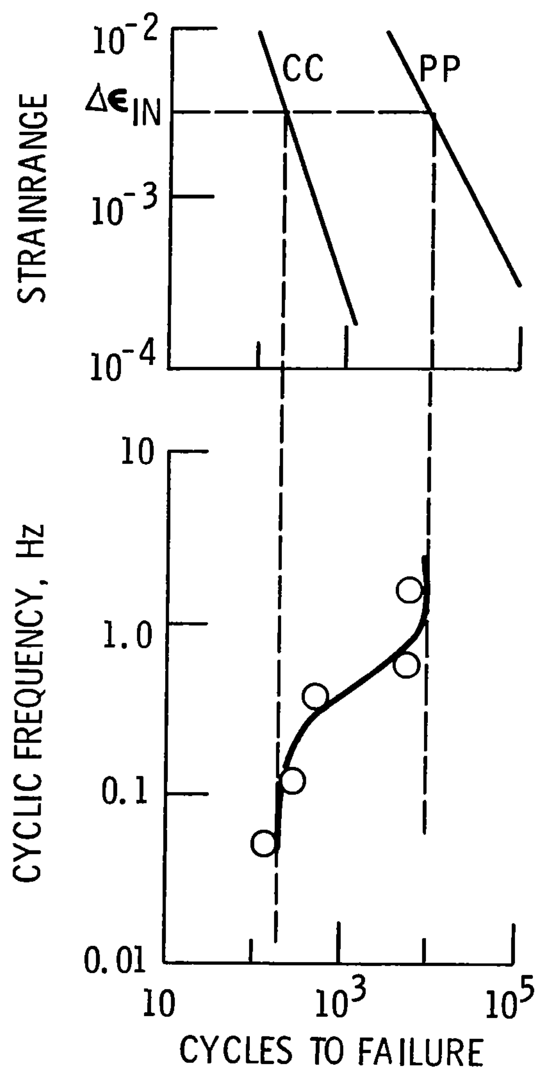

Figure 16

ESTIMATIONS FOR STRAINRANGE PARTITIONING LIFE RELATIONS

We realized that the SRP life relations may not be available for a particular material that a designer might be interested in using. We thus provided a procedure (ref. 7) for estimating the four SRP life relations from a knowledge only of materials tensile ductility D_P and creep ductility D_C. The constants in these equations were arrived at by correlating these measured ductilities with the SRP data for a large number of materials. There are two equations for the CP life relation. The first is to be used when the creep cracking is transcrystalline and the second is for when the cracking is intercrystalline. The life relations estimated by these equations, shown in figure 17, are in agreement with measured life relations to within a factor of approximately three in cyclic lifetime. The greater the ductility, the greater the resistance to failure by cyclic inelastic deformation. These equations also help to predict whether the SRP life relations are sensitive to test temperature. For example, if the ductility of an alloy does not change appreciably with temperature, it would be predicted that the SRP life relations would be insensitive to test temperature. This would be a distinct advantage in the analysis of thermal fatigue cycling with temperatures varying throughout the cycle. Two such materials that we have studied exhibit this desirable behavior. Results of our analyses of these materials are shown in the next figure.

$$\Delta\varepsilon_{PP} = 0.50\, D_P (N_{PP})^{-0.60}$$

$$\Delta\varepsilon_{PC} = 0.25\, D_P (N_{PC})^{-0.60}$$

$$\Delta\varepsilon_{CC} = 0.25 (D_C)^{0.60} (N_{CC})^{-0.60}$$

$$\Delta\varepsilon_{CP} = 0.20 (D_C)^{0.60} (N_{CP})^{-0.60} \quad \text{(TRANSCRYSTALLINE)}$$

$$\text{OR} \quad \Delta\varepsilon_{CP} = 0.10 (D_C)^{0.60} (N_{CP})^{-0.60} \quad \text{(INTERCRYSTALLINE)}$$

Figure 17

TEMPERATURE INSENSITIVITY OF SRP LIFE RELATIONS

The SRP life relations for two steels were measured at a single baseline test temperature appropriate to each (ref. 8), as indicated by the open circles in figure 18. Additional SRP-type test cycles, as indicated by the closed circles, were conducted at higher and lower test temperatures and their lives were predicted based upon the baseline SRP life relations. Since the ductilities for these materials did not vary appreciably over the temperature range studied, the SRP life relation also did not vary appreciably, and the predictions were therefore quite accurate, being within about a factor of two in cyclic lifetime.

It should be pointed out that although the life relations may not be functions of temperature, the stress-strain relationships and the creep rate versus stress relationships are still highly sensitive to temperature.

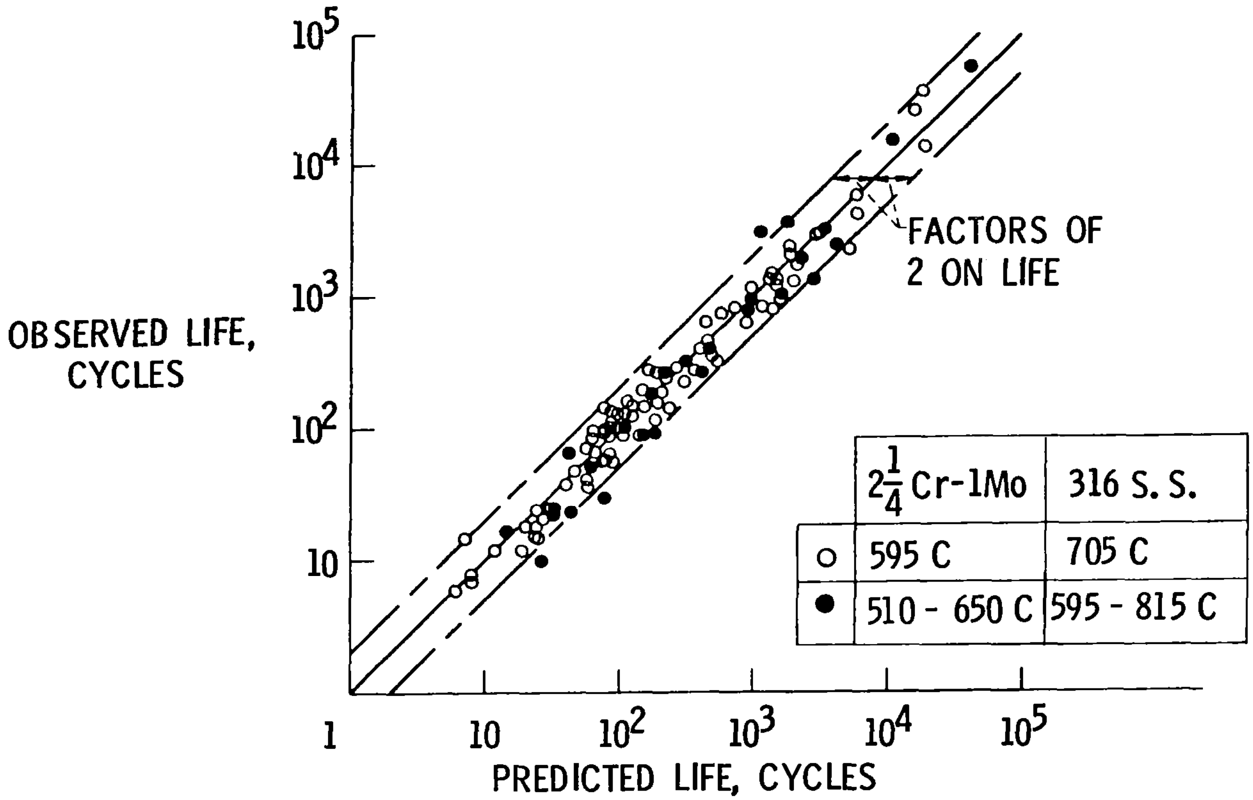

Figure 18

MULTIAXIAL EFFECTS

Multiaxial states of stress are known to affect the inelastic straining behavior of materials as well as their fatigue behavior. We have developed a two-step procedure to account for these multiaxial stress effects when using the Strainrange Partitioning Method.

We begin by determining the four SRP life relations from uniaxial tests. Referring to figure 19, the first step in dealing with a multiaxial stress state is to determine the Equivalent Inelastic Strainrange using the von Mises yield criteria. This takes care of the multiaxiality on the inelastic straining behavior. This is also called the flow or shear behavior. The second step is to determine the degree of hydrostatic stress present. If the hydrostatic stress is tensile, the life relations are decreased, but if the hydrostatic stress is compressive, the life relations are increased. Equations for making the required calculations are included in refs. 9 and 10. We have found the two-step approach to be more accurate than forcing a single multiaxial criterion to correlate uniaxial and multiaxial states of stress in fatigue.

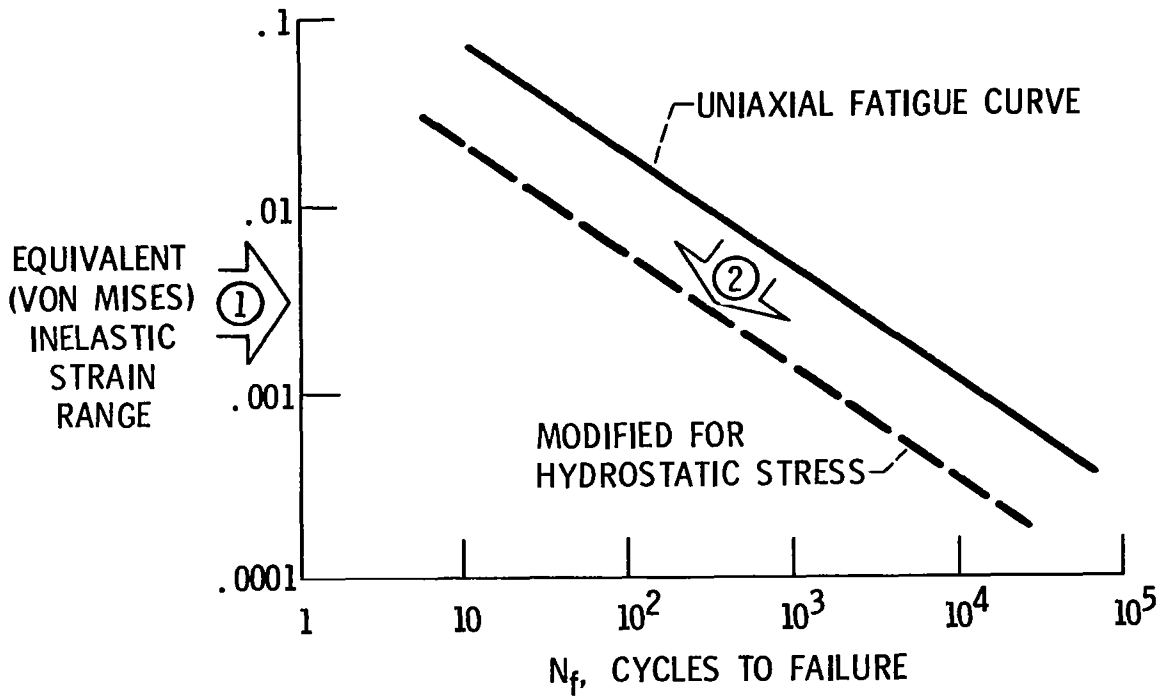

Figure 19

MEAN STRESS EFFECTS

Mean stresses may occur during low-cycle fatigue and thermal fatigue. Their damaging or beneficial influence must be determined in order to accurately predict cyclic lifetime. The effect of mean stresses on high-cycle fatigue life is well understood and established procedures exist for calculating their influence on life. These effects can be very large. However, in the low-cycle fatigue region, their effects are not as great, and at large enough strain ranges and low enough cyclic lives, the effect decreases to zero. This trend is shown in the figure. Here, in the high-cycle region, where the stress-strain response is linearly elastic, mean stresses have their full effect. Typically, compressive mean stresses improve life and tensile mean stresses decrease life. As shown schematically in figure 20, the mean stress effect decreases toward zero at the lower number of cycles to failure. We have developed a relatively simple procedure (ref. 11) for accounting for the effects of mean stress in the low- and intermediate-cycle fatigue region. This procedure is based upon the Morrow Equation for the Goodman diagram which was derived for high-cycle fatigue behavior.

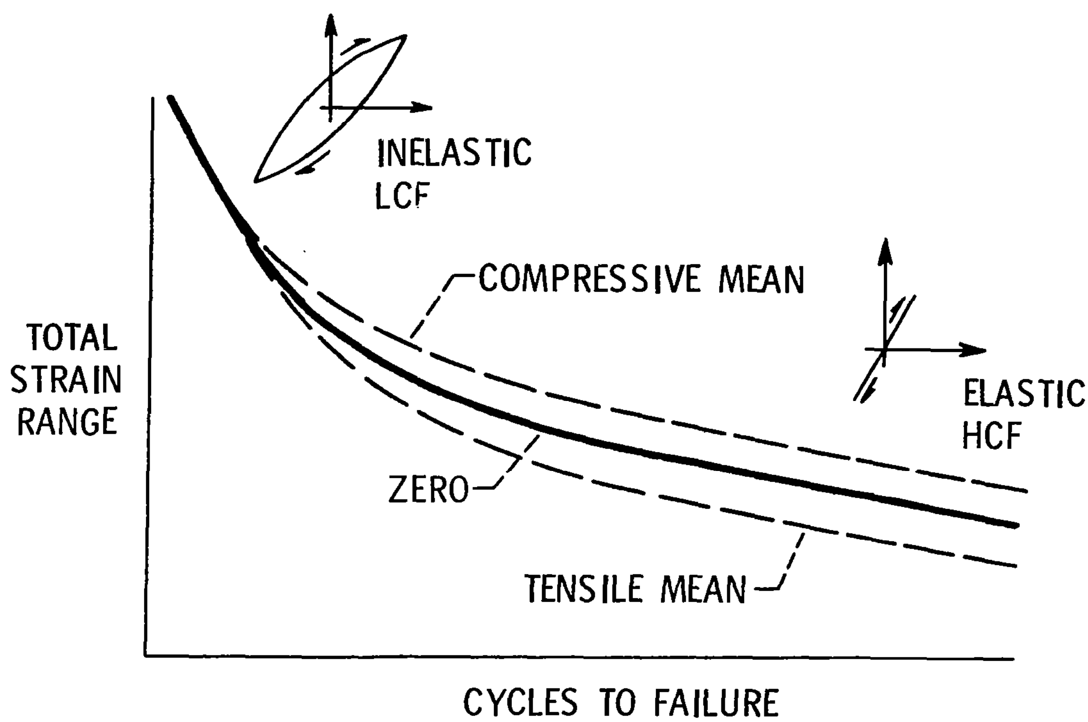

Figure 20

EFFECTIVE IMPLEMENTATION OF STRAINRANGE PARTITIONING

Up to this point in the presentation, I have discussed many of the details of the life prediction methods that have been developed at the NASA Lewis Research Center. I have concentrated mainly on the Method of Strainrange Partitioning. We do realize that to implement the method places a burden upon the materials engineer who must provide the necessary material characterization properties, and a similar burden is placed upon the structural analyst who must do a more thorough job of calculating the localized inelastic strains that occur in a high-temperature component part. For example, the materials engineer must determine the four SRP life relations for the material, and if these are functions of temperature, must determine them at enough isothermal temperatures to permit interpolation and extrapolation as needed. He must also provide the structural analyst with the cyclic constitutive equations that characterize the cyclic stress-strain-creep-time-temperature relations of the material. The structural analyst must then anticipate the thermal and mechanical loading on a component part, to identify the most critical locations where failures may originate, and then calculate the local stresses and strains. The inelastic strains must then be partitioned into their creep and plastic portions in order to predict a cyclic lifetime using Strainrange Partitioning.

If these advanced capabilities are available, then the Method of Strainrange Partitioning has many attributes that represent a vast improvement over previously proposed methods of life prediction.

ATTRIBUTES OF STRAINRANGE PARTITIONING

The method of Strainrange Partitioning is general enough to permit a thorough characterization of the creep-fatigue behavior of materials. As indicated in figure 21, the method is generic and applicable to any creep-fatigue cycle, including thermal mechanical cycling. It can provide upper and lower bounds on cyclic lifetime with a minimum of analysis, and it can readily account for the effects of such factors as: Frequency, Hold Time, Waveshape, Temperature, State of Stress, Mean Stress, and Strain Ratchetting.

Research is in progress for improving the applicability of the method to the solution of practical engineering design problems.

For example, some current research is focused on casting the method in terms of the total strainrange rather than just the inelastic strainrange.

Although considerable work has been done toward the development of the method, further research and development are needed to make the method a practical tool for routine analysis and life prediction of turbine engine hot section components.

In addition to SRP, there are a number of life prediction approaches under development by other research organizations. These include variations of the Time and Cycle Fraction Method, and other approaches that consider cyclic frequency or cyclic inelastic straining rate as the primary variables governing time-dependent damage accumulation. Since few of these address the problems of nonrepetitive cycles (i.e., cumulative fatigue cycling), we have recently researched procedures to deal with this phenomenon.

- CHARACTERIZES CREEP-FATIGUE BEHAVIOR OF ALLOYS
- PROVIDES BOUNDS OF CYCLIC LIFE
- PREDICTS EFFECTS OF:
  - FREQUENCY
  - HOLD TIME
  - WAVESHAPE
  - TEMPERATURE
  - STATE OF STRESS
  - RATCHETTING
- APPLICABLE TO ANY COMPLEX THERMAL-MECHANICAL STRAIN CYCLE

Figure 21

Simple procedures have been developed and verified (ref. 12) for treating the difficult problem of nonlinear cumulative fatigue crack initiation damage under complex loading histories. The Double Linear Damage Rule (DLDR) is a concept arrived at through viewing the fatigue process as two sequential phases: the first, Phase I, associated with microscopic changes in the surface layer of material being fatigued, and the second, Phase II, with the propagation of microcracks to the point that is classified as fatigue crack initiation on the macroscopic engineering level.

The application of the newly proposed rule involves two steps, each similar to the conventional application of the classical Miner Linear Damage Rule. When the sum of the cycle ratios based on Phase I lives reaches unity, Phase I is presumed complete, and further loadings are summed as cycle ratios based on Phase II lives. Once Phase II cycle ratios sum to unity, failure by macrocrack initiation is presumed to occur. No other physical properties or material constants than those normally required in a conventional Miner Linear Damage Rule analysis are required for application of the DLDR. Examples of the application of the approach are shown in figure 22.

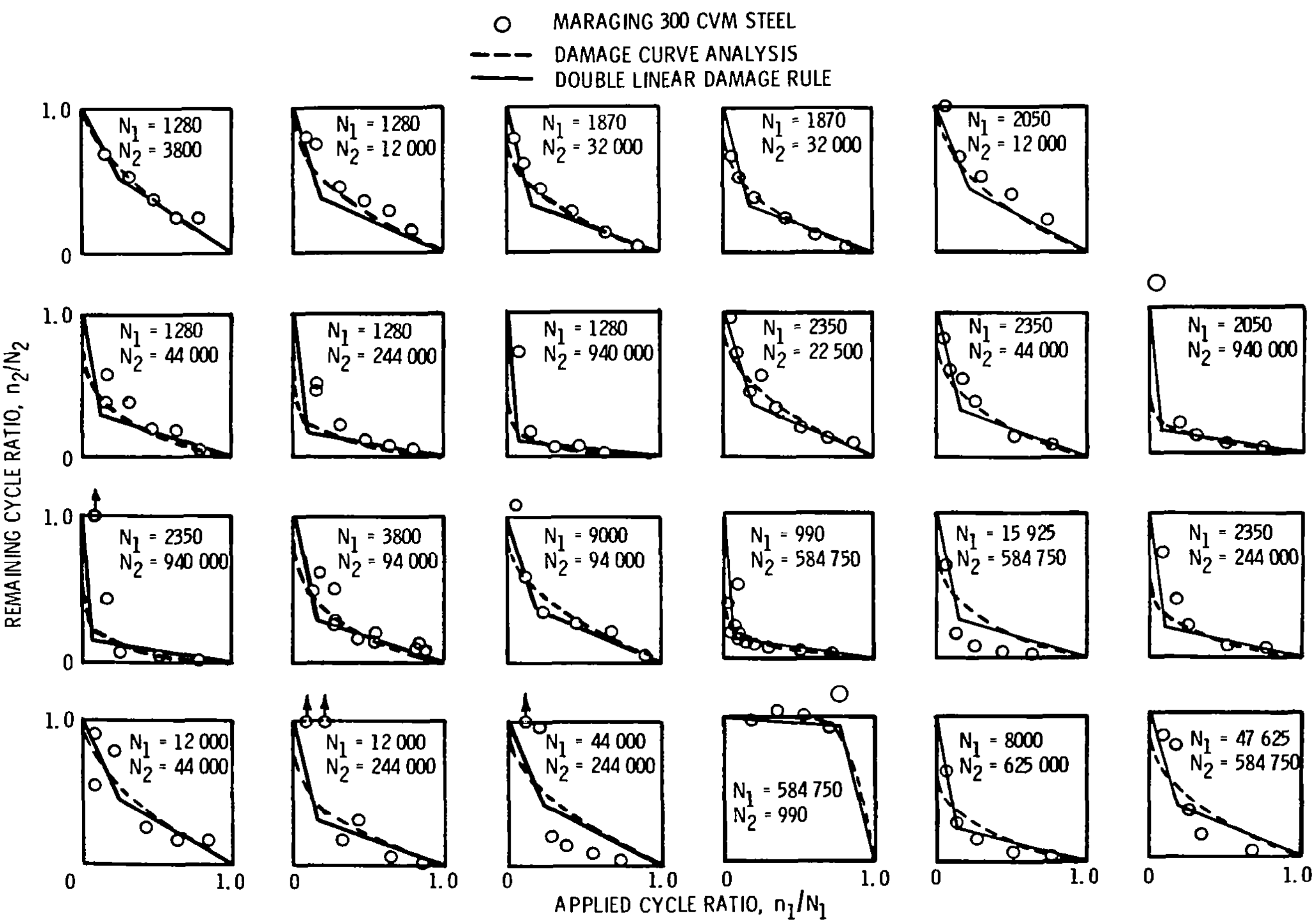

Figure 22

TURBINE COMPONENT LIFE PREDICTION

We have an intensive program aimed at generating the controlled experimental data needed for the development and verification of these life prediction methods. As shown in figure 23, we are using a variety of specimens ranging in complexity from the simple laboratory specimen to actual gas turbine engine components.

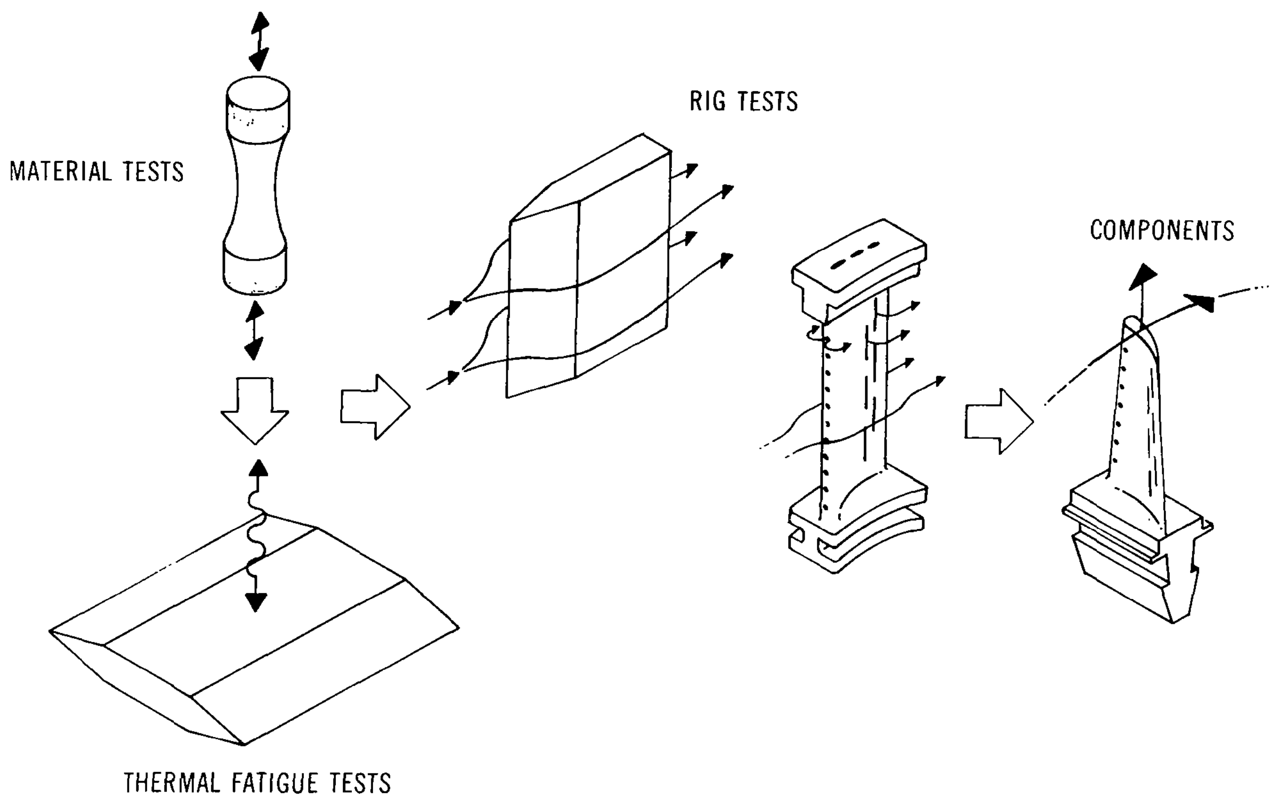

Figure 23

REFERENCES

1. Manson, S. S.: Behavior of Materials Under Conditions of Thermal Stress. NACA TN-2933, 1953.

2. Manson, S. S.: Fatigue: A Complex Subject - Some Simple Approximations. Exp. Mech., Vol. 5, No. 7, 1965, pp. 193-226.

3. Manson, S. S. and Halford, G. R.: A Method of Estimating High-Temperature Low-Cycle Fatigue Behavior of Materials. Proc. of Int. Conf. on Thermal & High-Strain Fatigue. Metals & Metallurgy Trust, London, 1967, pp. 154-170.

4. Taira, S.: Lifetime of Structures Subjected to Varying Load and Temperature. Creep in Structures, N. J. Hoff, ed.; Academic Press, New York, 1962, pp. 96-124.

5. Manson, S. S.; Halford, G. R.; and Spera, D. A.: The Role of Creep in High-Temperature Low-Cycle Fatigue. Advances in Creep Design, A. I. Smith & A. M. Nicolson, eds., Halsted Press, 1971, pp. 229-249.

6. Manson, S. S.; Halford, G. R.; and Hirschberg, M. H.: Creep-Fatigue Analysis by Strain-Range Partitioning. Symposium on Design for Elevated Temperature Environment, ASME, 1971, pp. 12-28. (NASA TM X-67838, 1971)

7. Halford, G. R.; Saltsman, J. F.; and Hirschberg, M. H.: Ductility Normalized-Strainrange Partitioning Life Relations for Creep-Fatigue Life Prediction. Proceedings of Conf. on Environmental Degradation of Engineering Materials. Virginia Tech Printing Dept., V.P.I. & State Univ., Blacksburg, VA, 1977, pp. 599-612.

8. Halford, G. R.; Hirschberg, M. H.; and Manson, S. S.: Temperature Effects on the Strainrange Partitioning Approach for Creep-Fatigue Analysis. STP 520, ASTM, 1973, pp. 658-669. (NASA TM X-68023, 1972)

9. Manson, S. S. and Halford, G. R.: Multiaxial Rules for Treatment of Creep-Fatigue Problems by Strainrange Partitioning. 1976 ASME-MPC Symposium on Creep-Fatigue Interaction, MPC-3, ASME, 1976, pp. 299-322. (NASA TM X-73488, 1976)

10. Manson, S. S. and Halford, G. R.: Discussion. Multiaxial Low-Cycle Fatigue of Type 304 Stainless Steel. Blass, J. J. and Zamrik, S. Y., 1976 ASME-MPC Symposium on Creep-Fatigue Interaction, MPC-3 ASME, 1976, pp. 129-159.

11. Halford, G. R. and Nachtigall, A. J.: The Strainrange Partitioning Behavior of an Advanced Gas Turbine Disk Alloy, AF2-1DA. J. Aircraft, Vol. 17, No. 8, 1980, pp. 598-604. (NASA TM-79179, 1979)

12. Manson, S. S. and Halford, G. R.: Practical Implementation of the Double-Linear Damage Rule & Damage Curve Approach for Treating Cumulative Fatigue Damage. Int. J. Fracture, Vol. 17, No. 2, 1981, pp. 169-192. Also, Vol. 17, No. 4, 1981, pp. R35-R42.